

The Madelung Problem of Finite Crystals

Yihao Zhao,^{1,2} Yang He,^{1,2} and Zhonghan Hu^{1,2,*}

¹Key Laboratory of Laser & Infrared System of Ministry of Education, Shandong University, Qingdao 266237, P. R. China

²Qingdao Institute for Theoretical and Computational Sciences (QITCS),

Center for Optics Research and Engineering, Shandong University, Qingdao 266237, P. R. China

The Coulomb potential at an interior ion in a finite crystal of size p is given by a linear superposition of contributions from displacement vectors $\mathbf{r} = (x, y, z)$ to its neighbors. This additive structure underlies universal relationships among Madelung constants and applies to both standard periodic boundary conditions and alternative Clifford supercells. Each pairwise contribution decomposes into three physically distinct components: a periodic bulk term, a quadratic boundary term, and a finite-size correction whose leading order term is $[24r^4 - 40(x^4 + y^4 + z^4)]/[9\sqrt{3}(2p + 1)^2]$ for cubic crystals with unit lattice constant. Combining this decomposition with linear superposition yields a rapidly convergent direct-summation scheme, accurate even at $p = 1$ (3^3 unit cells), enabling hands-on calculations of Madelung constants for a wide range of ionic crystals.

The classical Madelung problem concerns the electrostatic potential at the site of a reference ion in an infinite ionic crystal (e.g., NaCl or CsCl)[1]. When scaled by the potential of an isolated nearest-neighbor counterion, this defines the Madelung constant—a dimensionless quantity central to the lattice energy per ion pair. Its computation, however, is mathematically subtle: the conditionally convergent nature of the Coulomb series renders naive direct summation (e.g., over spherical or cubic shells) not only slow but also ambiguous, as the result may depend on the summation order[2, 3].

A rich literature has emerged to address this challenge. At one extreme lie highly accurate but analytically involved integral-transform methods—most notably Ewald summation and its related approaches[2, 4–6]. At the other are conceptually simpler direct-summation strategies: charge-renormalization schemes (e.g., Evjen’s surface-weighting[7], Harrison’s neutralizing shell[8], or multipole-cancellation approaches[9–12]) and geometric alternatives like the Clifford supercell (CS) method[13, 14], which redefines distances using the intrinsic metric of a Clifford torus.

TABLE I. Madelung constants for CsCl ($\mathbf{v}_1 = (0.5, 0.5, 0.5)$) computed using the explicitly corrected direct sum [Eqs. (1) to (3)] and the CS method [Eqs. (4) and (5)], for varying supercell sizes^a

p	$\sqrt{3}\nu_{\text{pbc}}(\mathbf{v}_1)/2$	abs. error	K	$\sqrt{3}\nu_{\text{CS}}(\mathbf{v}_1)/2$	abs. error
1	1.7629780255	3.0×10^{-4}	3	1.408794	-3.5×10^{-1}
5	1.7626721815	-2.6×10^{-6}	11	1.744082	-1.9×10^{-2}
20	1.7626747599	-1.3×10^{-8}	41	1.761379	-1.3×10^{-3}
60	1.7626747729	-1.7×10^{-10}	121	1.762526	-1.5×10^{-4}

^a The reference value is 1.76 267 477 307 098[15].

Yet truly analytical, hands-on computation remains elusive. For CsCl, Evjen’s method—reducing surface charges by 1/2, 1/4, and 1/8 on faces, edges, and corners—fails to converge to the correct value; Harrison’s neutralization—enforcing neutrality via a surrounding charged spherical shell—converges correctly but slowly, requiring radii of hundreds of lattice constants (i.e., millions of unit cells) to reach

$\sim 10^{-3}$ accuracy. While the multipole-cancellation scheme by Gelle and Lepetit achieves exponential convergence[12], it relies on increasingly intricate charge distributions that complicate practical implementation. The CS method, though conceptually simple and exhibiting $\mathcal{O}(K^{-2})$ convergence with a $K \times K \times K$ supercell, still demands $K \geq 40$ (tens of thousands of unit cells) for modest ($\sim 10^{-3}$) accuracy, as Tab. I illustrates.

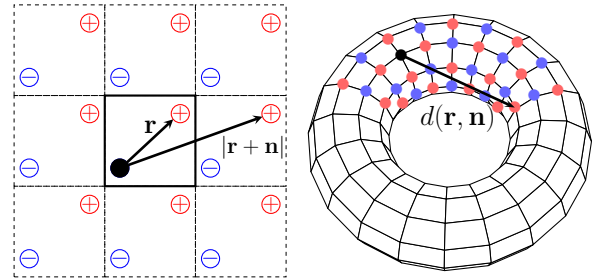


FIG. 1. Two-dimensional cross-sectional view of two particles with unit charges (± 1) separated by vector $\mathbf{r} = (x, y, z)$ and their periodic images under standard periodic boundary conditions (left) and in the CS method (right). For the conventional direct sum, the potential at the reference particle (black dot) is obtained by summing the Coulomb interactions $1/|\mathbf{r} + \mathbf{n}|$ from all periodic images, as described by Eq. (1). In the CS method (K^3 unit cells with unit side length), the conventional Euclidean distance $|\mathbf{r} + \mathbf{n}|$ is replaced by the renormalized distance $d(\mathbf{r}, \mathbf{n})$ (Eqs. (4) and (5)).

In this work, we overcome the slow convergence of conventional direct summation by incorporating higher-order multipolar effects via exact boundary and finite-size corrections—without resorting to charge or distance renormalization. For the CsCl-like two-particle configuration depicted in Fig. 1, the direct Coulomb sum for a finite crystal comprises of a shape- and size-independent bulk term $\nu_{\text{pbc}}(\mathbf{r})$, a size-independent boundary contribution $\nu_b(\mathbf{r}|\mathbf{s})$, and a finite-size correction $\nu_{\text{corr}}(\mathbf{r}, p|\mathbf{s})$

$$\nu(\mathbf{r}, p|\mathbf{s}) = \frac{1}{r} + \sum_{\mathbf{n} \neq 0}^{\mathcal{L}(p|\mathbf{s})} \left[\frac{1}{|\mathbf{r} + \mathbf{n}|} - \frac{1}{n} \right] , \quad (1)$$

$$= \nu_{\text{pbc}}(\mathbf{r}) + \nu_b(\mathbf{r}|\mathbf{s}) + \nu_{\text{corr}}(\mathbf{r}, p|\mathbf{s})$$

* zhonghanhu@sdu.edu.cn

where $\mathbf{r} = (x, y, z)$ denotes the relative displacement, $\mathbf{n} = (n_x, n_y, n_z)$ is the lattice vector, $n = |\mathbf{n}|$, and $\mathcal{L}(p|\mathbf{s})$ the set of all lattice vectors in a finite crystal of linear extent p (with $K = 2p + 1$ unit cells per dimension) and shape \mathbf{s} . The precise meaning of \mathbf{s} will be clarified later. In the present explicit finite-size correction (EC) method, the Madelung constant is obtained by isolating the bulk contribution ν_{pbc} from the direct sum $\nu(\mathbf{r}, p|\mathbf{s})$ and scaling it by the potential of an isolated counterion at the nearest-neighbor distance.

For a cubic crystal in a simple cubic lattice (lattice constants $l_x = l_y = l_z = 1$), the boundary and finite-size corrections admit closed-form expressions:

$$\nu_b(\mathbf{r}|\mathbf{s}) = -2\pi r^2/3, \quad (2)$$

and

$$\nu_{\text{corr}}(\mathbf{r}, p|\mathbf{s}) = \frac{24r^4 - 40(x^4 + y^4 + z^4)}{9\sqrt{3}(2p+1)^2} + \mathcal{O}(p^{-4}). \quad (3)$$

In contrast, the CS method employs the renormalized distance[13, 16]

$$d(\mathbf{r}, \mathbf{n}) = \frac{K}{\sqrt{2}\pi} \left[3 - \sum_{\alpha=1}^3 \cos \frac{2\pi(\mathbf{r} + \mathbf{n}) \cdot \mathbf{e}_\alpha}{K} \right]^{1/2}, \quad (4)$$

with \mathbf{e}_α the Cartesian unit vectors, and evaluates the bulk potential via the uncorrected direct sum

$$\nu_{\text{CS}}(\mathbf{r}) = \frac{1}{d(\mathbf{r}, \mathbf{0})} + \sum_{\mathbf{n} \neq \mathbf{0}}^{\mathcal{L}(p|\mathbf{0})} \left[\frac{1}{d(\mathbf{r}, \mathbf{n})} - \frac{1}{d(\mathbf{0}, \mathbf{n})} \right]. \quad (5)$$

As demonstrated in Tab. I for CsCl, incorporating Eqs. (2) and (3) accelerates convergence from $\mathcal{O}(K^{-2})$ (CS) to $\mathcal{O}(K^{-4})$ (EC). Remarkably, the EC method achieves 3×10^{-4} accuracy with the minimal supercell ($p = 1, K = 3$), and delivers nine-digit precision at $p = 60$ —all without renormalization.

TABLE II. Bulk contributions for displacement vectors $\mathbf{v}_2 = (0.5, 0, 0)$, $\mathbf{v}_3 = (0.5, 0.5, 0)$, and $\mathbf{v}_4 = (0.25, 0.25, 0.25)$ computed using the EC method and referenced to $p = 60$ result (nine significant digits).

p	$\nu_{\text{pbc}}(\mathbf{v}_2)$	$\nu_{\text{pbc}}(\mathbf{v}_3)$	$\nu_{\text{pbc}}(\mathbf{v}_4)$
1	2.741146342	2.255022524	2.636876604
5	2.741365130	2.254776731	2.636813436
20	2.741365174	2.254775952	2.636813487
ref.	2.741365175	2.254775948	2.636813487

Table II shows that, the correction scheme maintains high accuracy (better than 10^{-8} at $p = 20$) across a range of displacement vectors, confirming its robustness for arbitrary displacements. As detailed later, the two-ion configuration serves as a fundamental building block for the Madelung problem: for crystals with multi-atom unit cells (e.g., the crystal structures in Tab. III), the total Madelung constant is obtained by linearly superposing contributions from all

symmetry-inequivalent ion pairs, each evaluated via the direct sum in Eq. (1) and corrected analytically using $\nu_b + \nu_{\text{corr}}$. This additive property, combined with the $\mathcal{O}(p^{-4})$ convergence of every term, enables a truly analytical, renormalization-free evaluation of Madelung constants—even for complex ionic structures such as NaCl, ZnS, CaF₂ and CaTiO₃. In the following, we provide rigorous derivations of $\nu_b(\mathbf{r}|\mathbf{s})$ and $\nu_{\text{corr}}(\mathbf{r}, p|\mathbf{s})$ for a general orthogonal lattice. While $\nu_b(\mathbf{r}|\mathbf{s})$ admits a closed-form expression for crystals with arbitrary aspect ratios, the explicit closed-form expression $\nu_{\text{corr}}(\mathbf{r}, p|\mathbf{s})$ in Eq. (3) is derived for cubic crystals in a cubic lattice. Nevertheless, this formulation is sufficient to compute highly accurate Madelung constants for a broad set of benchmark structures—requiring only minimal computational effort.

It is well known that the Coulomb lattice sum is a conditionally convergent series whose value depends on the macroscopic shape of the crystal[2, 3]. A rigorous treatment therefore requires defining a sequence of finite crystals that grow in size while maintaining a fixed geometric shape. We consider an orthogonal lattice where the lattice constants l_x, l_y , and l_z represent the edge lengths of the orthorhombic unit cell. For a centro-symmetric crystal composed of one central primitive cell and N_1, N_2, N_3 replicated cells extending symmetrically along the $\pm x, \pm y$, and $\pm z$ -directions, respectively, the position of each unit cell is specified by the lattice vector

$$\mathbf{n} = (n_x, n_y, n_z) = (n_1 l_x, n_2 l_y, n_3 l_z), \quad (6)$$

where n_1, n_2, n_3 are integers in the range $-N_\alpha \leq n_\alpha \leq N_\alpha$ for $\alpha = 1, 2, 3$. The overall dimensions of the resulting cuboid are therefore $a = (2N_1 + 1)l_x$, $b = (2N_2 + 1)l_y$, and $c = (2N_3 + 1)l_z$.

In the isotropic case where $N_1 = N_2 = N_3 = p$, the crystal retain the same aspect ratios as the primitive cell:

$$a : b : c = l_x : l_y : l_z. \quad (7)$$

Thus, as p increases from zero, the sequence of crystals maintains a fixed shape under isotropic growth.

For the general anisotropic case, we define an effective size p such that $2p + 1$ equals the greatest common divisor of $2N_1 + 1, 2N_2 + 1$ and $2N_3 + 1$. This condition implies the simultaneous factorizations:

$$2N_\alpha + 1 = (2s_\alpha + 1)(2p + 1) \quad \text{for } \alpha = 1, 2, 3, \quad (8)$$

where the quotients $(2s_1 + 1, 2s_2 + 1, 2s_3 + 1)$ form a co-prime triplet—i.e., their only common divisor is 1. As p increases with fixed $\mathbf{s} = (s_1, s_2, s_3)$, the crystal dimensions evolve as: $a = (2p + 1)(2s_1 + 1)l_x$, $b = (2p + 1)(2s_2 + 1)l_y$, and $c = (2p + 1)(2s_3 + 1)l_z$, giving invariant aspect ratios:

$$a : b : c = (2s_1 + 1)l_x : (2s_2 + 1)l_y : (2s_3 + 1)l_z. \quad (9)$$

Consequently, all crystals in this sequence maintain an identical geometric shape, uniquely specified by the parameter \mathbf{s} for any given set of lattice constants (l_x, l_y, l_z) .

Now, suppose each unit cell consists of M ions with charges q_j located at positions \mathbf{r}_j for $j = 1, 2, \dots, M$. The

TABLE III. Reduced coordinates of ions in a cubic unit cell of a typical rocksalt (Na_4Cl_4), zincblende (Zn_4S_4) and fluorite (Ca_4F_8), with the unit cell scaled to unit length: $l_x = l_y = l_z = 1$.

$4\text{Na}^+/4\text{Ca}^{2+}$	$4\text{Cl}^-/4\text{Zn}^{2+}$	$4\text{S}^{2-}/4\text{F}^-$	4F^-
$(0, 0, 0)(0.5, 0, 0.5)$	$(0.5, 0, 0)(0, 0.5, 0)$	$(0.25, 0.25, 0.25)(0.75, 0.25, 0.75)$	$(0.25, 0.25, 0.75)(0.25, 0.75, 0.25)$
$(0.5, 0.5, 0)(0, 0.5, 0.5)$	$(0, 0, 0.5)(0.5, 0.5, 0.5)$	$(0.75, 0.75, 0.25)(0.25, 0.75, 0.75)$	$(0.75, 0.25, 0.25)(0.75, 0.75, 0.75)$

electric potential at the i -th ion in the primary cell ($\mathbf{n} = \mathbf{0}$) is then given by

$$\phi_p(i) = \sum_{j=1, j \neq i}^M \frac{q_j}{|\mathbf{r}_j - \mathbf{r}_i|} + \sum_{j=1}^M \sum_{\mathbf{n} \neq \mathbf{0}} \frac{q_j}{|\mathbf{r}_j + \mathbf{n} - \mathbf{r}_i|}. \quad (10)$$

This expression—and analogous sums for the electrostatic energy—constitutes the starting point for deriving the Ewald summation and the associated shape-dependent boundary contributions in the limit of a macroscopic (infinite) crystal (e.g.[2, 3, 17, 18]). In contrast, we rigorously define the geometry of finite crystals for a general orthogonal lattice, thereby enabling a transparent and systematic treatment of finite-size effects. In the absence of such a formulation, the boundary contribution in the infinite limit remains ambiguous—often obscured by implicit assumptions and lacking direct justification from finite, physically realizable systems.

Under the condition of charge neutrality, $\sum_{j=1}^M q_j = 0$, the self-interaction part ($i = j$) in the second sum can be rewritten as

$$\sum_{\mathbf{n} \neq \mathbf{0}} \frac{q_i}{|\mathbf{n}|} = - \sum_{j=1, j \neq i}^M \sum_{\mathbf{n} \neq \mathbf{0}} \frac{q_j}{|\mathbf{n}|}, \quad (11)$$

allowing the potential to be recast in a pairwise form[18–20]

$$\phi_p(i) = \sum_{j=1, j \neq i}^M q_j \nu(\mathbf{r}_j - \mathbf{r}_i, p|\mathbf{s}), \quad (12)$$

where the effective pairwise interaction $\nu(\mathbf{r}, p|\mathbf{s})$ is defined in Eq. (1).

In prior work, the infinite-system limit of this interaction is decomposed as[18–20]

$$\nu(\mathbf{r}, \infty|\mathbf{s}) = \nu_{\text{pbc}}(\mathbf{r}) + \nu_b(\mathbf{r}|\mathbf{s}), \quad (13)$$

where $\nu_{\text{pbc}}(\mathbf{r})$ is geometry-independent and represents the bulk contribution under periodic boundary conditions (PBC). This term has served as a foundation for analytical studies of structural correlations in bulk electrolytes and dielectrics[21, 22], as well as dielectric responses at interfaces[23, 24]. The second term, $\nu_b(\mathbf{r}|\mathbf{s})$ accounts for the arrangement of charges at the infinite boundary[20]. Crucially, as we demonstrate below, it remains a non-negligible contribution even for finite crystals. In reciprocal space, it can be expressed as[18, 20]

$$\nu_b(\mathbf{r}|\mathbf{s}) = -\frac{2\pi}{V} \lim_{\mathbf{k}|\mathbf{s} \rightarrow 0} \frac{(\mathbf{k} \cdot \mathbf{r})^2}{|\mathbf{k}|^2}, \quad (14)$$

where $V = l_x l_y l_z$ is the volume of a unit cell and the limit is taken such that the wavevector \mathbf{k} approaches zero along a direction determined by the aspect ratios encoded in \mathbf{s} . This

representation makes manifest that $\nu_b(\mathbf{r}|\mathbf{s})$ is always non-positive. Equivalently, in real space, $\nu_b(\mathbf{r}|\mathbf{s})$ admits an electrostatic interpretation: it is the interaction energy between a point dipole at the origin and a uniformly polarized continuum filling the crystal volume[17, 20, 25, 26]:

$$\nu_b(\mathbf{r}|\mathbf{s}) = \frac{1}{2V} \int_{\Omega(p|\mathbf{s})} d\mathbf{x} (\mathbf{r} \cdot \nabla_{\mathbf{x}})^2 \frac{1}{|\mathbf{x}|}, \quad (15)$$

where the integration domain $\Omega(p|\mathbf{s})$ denotes the total volume of the crystal:

$$\Omega(p|\mathbf{s}) = abc = V(2p+1)^3 \prod_{\alpha=1}^3 (2s_{\alpha}+1). \quad (16)$$

Notably, although this domain depends on p , explicit evaluation [see Supporting Information (SI)] yields a closed-form, p -independent expression:

$$\nu_b(\mathbf{r}|\mathbf{s}) = -\frac{4}{V} \sum_{\alpha=1}^3 \frac{(\mathbf{r} \cdot \mathbf{e}_{\alpha})^2}{\xi_{\alpha}^2} \text{atan} \frac{1}{\sqrt{\xi_1^2 + \xi_2^2 + \xi_3^2}}, \quad (17)$$

where $\text{atan}(\cdot)$ is the inverse tangent function and the dimensionless parameter ξ_{α} are defined by normalizing each side length with the geometric mean of the three:

$$\xi_1 = \frac{a}{(abc)^{1/3}}; \quad \xi_2 = \frac{b}{(abc)^{1/3}}; \quad \xi_3 = \frac{c}{(abc)^{1/3}}. \quad (18)$$

For a cubic crystal with unit lattice constant ($l_x = l_y = l_z = 1$), $\nu_b(\mathbf{r}|\mathbf{s})$ of Eq. (17) simplifies to Eq. (2).

For a finite crystal of size p , the effective pairwise interaction $\nu(\mathbf{r}, p|\mathbf{s})$ deviates from $\nu(\mathbf{r}, \infty|\mathbf{s})$ by the finite-size correction $\nu_{\text{corr}}(\mathbf{r}, p|\mathbf{s})$ introduced in Eq. (1). $\nu_{\text{corr}}(\mathbf{r}, p|\mathbf{s})$ accounts for the omitted contributions from lattice vectors outside the finite summation domain. Explicitly,

$$\nu_{\text{corr}}(\mathbf{r}, p) = - \sum_{\mathbf{n} \notin \mathcal{L}(p|\mathbf{s})} \left[\frac{1}{|\mathbf{r} + \mathbf{n}|} - \frac{1}{n} \right], \quad (19)$$

with the sum extending over all lattice vectors excluded from the finite crystal but present in the infinite lattice of the same shape.

To estimate $\nu_{\text{corr}}(\mathbf{r}, p|\mathbf{s})$ to a desired accuracy, we expand the summand for distant cells ($r \ll n$) as a multipolar series:

$$\frac{1}{|\mathbf{r} + \mathbf{n}|} - \frac{1}{n} = \sum_{k=1}^{\infty} \frac{(-r)^k P_k(\cos \theta)}{n^{k+1}} = \sum_{k=1}^{\infty} \frac{(\mathbf{r} \cdot \nabla_{\mathbf{n}})^k}{k!} \frac{1}{n}, \quad (20)$$

where $\cos \theta = \mathbf{r} \cdot \mathbf{n} / (nr)$, $P_k(\cos \theta)$ is the k -th Legendre polynomial, and $\nabla_{\mathbf{n}}$ is the gradient operator with respect to the lattice vector \mathbf{n} . Gelle and Lepetit performed a similar multipole

expansion using spherical coordinates rather than Cartesian coordinates[12]. Their approach facilitates asymptotic estimation of truncation errors and analysis of convergence behavior. In contrast, we derive exact leading-order terms of $\nu_{\text{corr}}(\mathbf{r}, p|\mathbf{s})$ directly in Cartesian coordinates.

Because $P_k(\cos \theta)$ is odd in \mathbf{n} for odd k , contributions from lattice vectors $\pm \mathbf{n}$ cancel in Eq. (19); hence, only even-order multipoles ($k = 2, 4, \dots$) survive. For instance, the $k = 2$ (dipolar) contribution reads

$$\begin{aligned} & \sum_{\mathbf{n} \notin \mathcal{L}(p|\mathbf{s})}^{\mathcal{L}(\infty|\mathbf{s})} \frac{n^2 r^2 - 3(\mathbf{n} \cdot \mathbf{r})^2}{2n^5} \\ &= \sum_{\mathbf{n} \notin \mathcal{L}(p|\mathbf{s})}^{\mathcal{L}(\infty|\mathbf{s})} \frac{n^2 r^2 - 3(x^2 n_x^2 + y^2 n_y^2 + z^2 n_z^2)}{2n^5}, \quad (21) \end{aligned}$$

where the cross terms in the expansion of $(\mathbf{n} \cdot \mathbf{r})^2$ vanish upon summation because of the odd symmetry under $n_\alpha \rightarrow -n_\alpha$. In general, the k -th (k even) multipole contributes a combination of terms such as $x^k, y^k, x^{k-2}y^2$, etc., with coefficients determined by the shape and size of the crystal. Their scaling behavior can be obtained via asymptotic analysis. For $r \ll n$, the discrete sum in Eq. (19) may be approximated by a continuous integral over the excluded volume $\Omega(\infty|\mathbf{s}) - \Omega(p|\mathbf{s})$ —the region between two similarly shaped cuboids (same aspect ratios, differing only in scale)—with a lattice-point density $1/V$. In this continuum picture, the k -th multipole in the integrand decays as $n^{-(k+1)}$, while the excluded volume grows as p^3 , suggesting a naive $\mathcal{O}(p^{2-k})$ scaling.

Crucially, for $k = 2$ (dipolar), the continuum integral over a cuboid depends only on its shape—not its absolute size [see Eq. (17)]. Since $\Omega(\infty|\mathbf{s})$ and $\Omega(p|\mathbf{s})$ share identical aspect ratios, this continuum integral over the excluded volume vanishes exactly. Thus, the leading dipolar contribution arises solely from the discreteness of the lattice and decays as $\mathcal{O}(p^{-2})$. This residual dipolar term, together with the $\mathcal{O}(p^{-2})$ continuum contribution from the $k = 4$ (quadrupolar) term, constitutes the total leading-order finite-size correction of order p^{-2} . Therefore, for a general orthogonal lattice, isolating the closed-form $\nu_b(\mathbf{r}|\mathbf{s})$ in Eq. (17) from the direct sum over a finite crystal of size p yields a bulk estimate whose accuracy matches that of the CS method—without introducing renormalization.

This clean separation between boundary (shape-dependent, p -independent) and finite-size (p -dependent) corrections relies fundamentally on using cuboid-shaped finite crystals aligned with the orthogonal lattice vectors. Such domains are self-similar under uniform scaling, enabling the exact cancellation of shape-dependent integrals over the excluded volume. In contrast, spherical or ellipsoidal crystals—typically constructed by removing unit cells near corners and edges—lack strict shape similarity between the finite and infinite reference domains. Consequently, the dipolar integral over the excluded region no longer vanishes, entangling boundary and finite-size effects.

While a closed-form expression for the $\mathcal{O}(p^{-2})$ finite-size correction remains challenging for a general orthogonal lat-

tice, it can be derived explicitly for the cubic case—where the crystal ($a = b = c$) and lattice ($l_x = l_y = l_z$) share cubic symmetry and $\mathbf{s} = \mathbf{0}$. Cubic symmetry enforces

$$\sum_{\mathbf{n} \notin \mathcal{L}(p|\mathbf{0})}^{\mathcal{L}(\infty|\mathbf{0})} \frac{3n_x^2}{n^5} = \sum_{\mathbf{n} \notin \mathcal{L}(p|\mathbf{0})}^{\mathcal{L}(\infty|\mathbf{0})} \frac{1}{n^3}, \quad (22)$$

and analogously for n_y^2 and n_z^2 . As a result, both the continuum approximation and the residual discrete dipolar terms vanish. Interestingly, Eq. (22) also holds for spherical truncation of cubic unit cells. Hence, the leading correction in both cubic and spherical crystals with $l_x = l_y = l_z$ stems solely from the $k = 4$ multipole. In the SI, we evaluate the corresponding continuum integral explicitly for cubic crystals, obtaining the closed-form expression given in Eq. (3). Such a closed-form expression for the spherical case, however, remains unknown.

TABLE IV. Madelung constants ($p = 20$ or $K = 41$) for representative ionic crystals: NaCl (rocksalt), ZnS (zincblende), and CaF₂ (fluorite).

method	NaCl	ZnS	F ⁻
CS	1.7479628535	1.638065778	0.4114803724
EC	1.7475645804	1.638055048	0.4124341357
ref.	1.7475645946	1.638055053	0.4124341357

We have now derived both the boundary and finite-size corrections to the direct sum. This analysis shows that the boundary correction $\nu_b(\mathbf{r}|\mathbf{s})$ has a dipolar character and is independent of crystal size p , whereas the leading finite-size correction $\nu_{\text{corr}}(\mathbf{r}|\mathbf{s})$ scales as p^{-2} . In general, this p^{-2} scaling arises from both a residual dipolar contribution and a continuum quadrupolar contributions; for the cubic case, however, it stems solely from the quadrupolar term. Notably, while the periodic part $\nu_{\text{pbc}}(\mathbf{r})$ is invariant under lattice translation, neither the boundary contribution ν_b , the finite-size correction ν_{corr} , nor the direct sum itself shares this periodicity. Consequently, evaluating these three terms at a periodically translated displacement might improve the accuracy of the bulk estimate, particularly for small p .

In practice, many ionic crystals adopt a cubic conventional unit cell; fractional coordinates for several examples are listed in Tab. III. For such systems, the electrostatic potential—and hence the Madelung constant—can be constructed by a linear superposition of pairwise bulk contributions $\nu_{\text{pbc}}(\mathbf{r})$ over all symmetry-inequivalent displacements between ion pairs.

To compute Madelung constants for NaCl, ZnS, CaF₂ and CaTiO₃, we employ four displacement vectors. One is $\mathbf{v}_1 = (0.5, 0.5, 0.5)$ as in CsCl; the others ($\mathbf{v}_2, \mathbf{v}_3$, and \mathbf{v}_4) and their corresponding ν_{pbc} value are given in Tab. II. Using Eq. (12), the Madelung constants reported in Tables IV and V are obtained by summing the appropriately weighted $\nu_{\text{pbc}}(\mathbf{v}_j)$ terms, each analytically corrected via ν_b and ν_{corr} . With $p = 20$, nine-digit accuracy is achieved, consistent with the precision of ν_{pbc} itself. This $\mathcal{O}(p^{-4})$ EC approach therefore surpasses the CS approach for all cubic lattices investigated.

TABLE V. Electrostatic energies of ions and a formula unit in a bulk CaTiO₃ crystal, where the fraction coordinates are: Ca²⁺ at (0.5, 0.5, 0.5), Ti⁴⁺ at (0, 0, 0), and O²⁻ at (0.5, 0, 0), (0, 0.5, 0), and (0, 0, 0.5).^a

ions	$p = 20$	ref.
Ca ²⁺	-2.693604868	-2.693604825
Ti ⁴⁺	-12.37746806	-12.37746803
O ²⁻	-3.227954396	-3.227954401
cell	-24.75493611	-24.75493606

^a Energies are normalized by e^2/d^2 , where d is the distance between the nearest Ti⁴⁺-O²⁻ pair.

The necessity and magnitude of these corrections depend critically on the multipole character of the unit cell. For CsCl, the unit cell possesses a large dipole moment, yielding a boundary contribution of $\pi |\mathbf{v}_1|^2 / \sqrt{3} = \sqrt{3}\pi/4 \simeq 1.36$, which dominates the final reference value; the remaining finite-size correction [e.g. $-\sqrt{3}\nu_{\text{corr}}(\mathbf{v}_1, 1|\mathbf{0})/2 \simeq -0.037$] and the direct sums (e.g. $\simeq 0.44$ at $p = 1$) are relatively small. Similarly, for ZnS, CaF₂, and CaTiO₃, significant dipole and quadrupole moments exist, necessitating explicit corrections to the direct sums.

In contrast, the cubic (NaCl)₄ unit cell forms an octopolar

configuration with vanishing dipole and quadrupole moments:

$$\sum_{j=1}^8 q_j x_{ij}^2 = \sum_{j=1}^8 q_j x_{ij}^4 = 0, \quad (23)$$

and analogously for y and z . Consequently, as noted in earlier work (e.g., Refs.[13, 20, 27]), various direct summation schemes without explicit corrections already yield accurate Madelung constants for NaCl. Interestingly, the CS method performs worse than these direct sums for NaCl; its correction cannot be simply ascribed to dipolar or quadrupolar contributions alone. Because the renormalized distance [Eq. (4)] depends on crystal size, it is difficult to approximate the leading order correction as an integral, making the finite-size effect harder to rationalize within the CS approach.

In summary, we have conducted a systematic analysis of the Madelung problem for finite crystals within a general orthogonal lattice. Our work resolves a conceptual ambiguity by cleanly separating the boundary correction from finite-size corrections in the direct summation. The resulting closed-form boundary correction provides an accurate method for computing Madelung constants with $\mathcal{O}(p^{-2})$ precision. For cubic lattices, where explicit closed-form expressions for both the boundary and the leading finite-size corrections are available, the approach achieves $\mathcal{O}(p^{-4})$ accuracy. Even with minimal supercells—corresponding to $p = 1$ (i.e., 3³ unit cells)—practical calculations already attain accuracy on the order of 10^{-4} , demonstrating applicability to ionic crystals such as NaCl, ZnS, CaF₂ and CaTiO₃.

This work was supported by NSFC (Grant Nos. 22273047 and 21873037).

[1] E. Madelung, “Die electrostatische untersuchung des kristallgitters,” *Phys. Z.* **19**, 524–533 (1918).

[2] S. W. de Leeuw, J. W. Perram, and E. R. Smith, “Simulation of electrostatic systems in periodic boundary conditions. i. lattice sums and dielectric constants,” *Proc. R. Soc. London, Ser. A Math. Phys. Sci.* **373**, 27–56 (1980).

[3] E. R. Smith, “Electrostatic energy in ionic crystals,” *Proc. R. Soc. London, Ser. A Math. Phys. Sci.* **375**, 475 (1981).

[4] P. P. Ewald, “Evaluation of optical and electrostatic lattice potentials,” *Ann. Phys. Leipzig* **64**, 253–287 (1921).

[5] F. W. Nijboer, B. R. A. and De Wette, “On the calculation of lattice sums,” *Physica* **23**, 309–321 (1957).

[6] D. Borwein, J. M. Borwein, and K. F. Taylor, “Convergence of lattice sums and madelung’s constant,” *J. Math. Phys.* **26**, 2999–3009 (1985).

[7] H. M. Evjen, “On the stability of certain heteropolar crystals,” *Phys. Rev.* **39**, 675–687 (1932).

[8] W. A. Harrison, “Simple calculation of madelung constants,” *Phys. Rev. B* **73**, 212103 (2006).

[9] V. R. Marathe, S. Lauer, and A. X. Trautwein, “Electrostatic potentials using direct-lattice summations,” *Phys. Rev. B* **27**, 5162–5165 (1983).

[10] C. Sousa, J. Casanovas, J. Rubio, and F. Illas, “Madelung fields from optimized point charges for ab initio cluster model calculations on ionic systems,” *J. Comput. Chem.* **14**, 680–684 (1993).

[11] S. E. Derenzo, M. K. Klintenberg, and M. J. Weber, “Determining point charge arrays that produce accurate ionic crystal fields for atomic cluster calculations,” *J. Chem. Phys.* **112**, 2074–2081 (2000).

[12] A. Gellé and M.-B. Lepetit, “Fast calculation of the electrostatic potential in ionic crystals by direct summation method,” *J. Chem. Phys.* **128**, 244716 (2008).

[13] N. Tavernier, G. Bendazzoli, V. Brumas, S. Evangelisti, and J. A. Berger, “Clifford boundary conditions: A simple direct-sum evaluation of madelung constants,” *J. Phys. Chem. Lett.* **11**, 7090–7095 (2020).

[14] N. Tavernier, G. L. Bendazzoli, V. Brumas, S. Evangelisti, and T. Leininger, “Clifford boundary conditions for periodic systems: the Madelung constant of cubic crystals in 1, 2 and 3 dimensions,” *Theor. Chem. Acc.* **140**, 106 (2021).

[15] [Http://oeis.org/A181152](http://oeis.org/A181152), Madelung Constant for CsCl Structure, The Online Encyclopedia of Integer Sequences.

[16] E. de Aragão, D. Moreno, S. Battaglia, G. Bendazzoli, S. Evangelisti, T. Leininger, N. Suaud, and J. A. Berger, “A simple position operator for periodic systems,” *Phys. Rev. B* **99**, 205145 (2019).

[17] V. Ballenegger, “Communication: On the origin of the surface term in the ewald formula,” *J. Chem. Phys.* **140**, 161102 (2014).

[18] Z. Hu, “Infinite boundary terms of ewald sums and pairwise in-

teractions for electrostatics in bulk and at interfaces," *J. Chem. Theory Comput.* **10**, 5254–5264 (2014).

[19] S. Yi, C. Pan, and Z. Hu, "Note: A pairwise form of the ewald sum for non-neutral systems," *J. Chem. Phys.* **147**, 126101 (2017).

[20] Y. Zhao and Z. Hu, "Infinite boundary terms and pairwise interactions: A unified framework for periodic coulomb systems," *J. Chem. Theory Comput.* **21**, 5916–5927 (2025).

[21] Z. Hu, "The symmetry-preserving mean field condition for electrostatic correlations in bulk," *J. Chem. Phys.* **156**, 034111 (2022).

[22] W. Gao, Z. Hu, and Z. Xu, "A screening condition imposed stochastic approximation for long-range electrostatic correlations," *J. Chem. Theory Comput.* **19**, 4822–4827 (2023).

[23] C. Pan, S. Yi, and Z. Hu, "The effect of electrostatic boundaries in molecular simulations: symmetry matters," *Phys. Chem. Chem. Phys.* **19**, 4861 (2017).

[24] C. Pan, S. Yi, and Z. Hu, "Analytic theory of finite-size effects in supercell modelling of charged interfaces," *Phys. Chem. Chem. Phys.* **21**, 14858 (2019).

[25] E. R. Smith, "Electrostatic potentials in systems periodic in one, two, and three dimensions," *J. Chem. Phys.* **128**, 174104 (2008).

[26] C. Pan, *A study on electrostatics algorithms in molecular simulations*, Ph.D. thesis, Jilin University (2017), pages 139–140.

[27] D. Wolf, "Reconstruction of nacl surfaces from a dipolar solution to the madelung problem," *Phys. Rev. Lett.* **68**, 3315–3318 (1992).

SUPPORTING INFORMATION

This Supporting Information presents explicit evaluations of the two integrals over centro-symmetric domains: a general cuboid $\Omega(a, b, c) = [-a/2, a/2] \times [-b/2, b/2] \times [-c/2, c/2]$ and a cube $\Omega(a, a, a) = [-a/2, a/2]^3$. Up to a multiplicative factor of $V = l_x l_y l_z$ (the volume of the unit cell), these integrals correspond to the infinite boundary term and the quadrupolar correction, respectively. The results are as follows:

$$I_1(\mathbf{r}, a, b, c) = \frac{1}{2} \int_{\Omega(a,b,c)} d\mathbf{x} (\mathbf{r} \cdot \nabla_{\mathbf{x}})^2 \frac{1}{|\mathbf{x}|} \\ = -4 \sum_{\alpha=1}^3 (\mathbf{r} \cdot \mathbf{e}_{\alpha})^2 \text{atan} \frac{1}{\xi_{\alpha}^2 \sqrt{\xi_1^2 + \xi_2^2 + \xi_3^2}}, \quad (\text{S1})$$

and

$$I_2(\mathbf{r}, a) = \frac{1}{24} \int_{[-a/2, a/2]^3} d\mathbf{x} (\mathbf{r} \cdot \nabla_{\mathbf{x}})^4 \frac{1}{|\mathbf{x}|}, \\ = \frac{24r^4 - 40(x^4 + y^4 + z^4)}{9\sqrt{3}a^2}, \quad (\text{S2})$$

where $\mathbf{x} = (x_1, x_2, x_3)$ is the integration variable, and $\mathbf{r} = (x, y, z)$ is a given vector with $r^2 = x^2 + y^2 + z^2$. In Eq. (S1), $\mathbf{e}_1, \mathbf{e}_2$, and \mathbf{e}_3 denote the orthogonal unit vectors along the x, y, z directions, respectively, so that $\mathbf{r} \cdot \mathbf{e}_1 = x$, etc. The dimensionless parameters ξ_{α} characterize the shape of the cuboid and are defined by normalizing each side length with the geo-

metric mean $(abc)^{1/3}$:

$$\xi_1 = \frac{a}{(abc)^{1/3}}; \quad \xi_2 = \frac{b}{(abc)^{1/3}}; \quad \xi_3 = \frac{c}{(abc)^{1/3}}, \quad (\text{S3})$$

which satisfy $\xi_1 \xi_2 \xi_3 = 1$. These parameters depend only on the relative proportions $a : b : c$, not the overall size of the cuboid. The function $\text{atan}(\cdot)$ in Eq. (S1) denotes the inverse tangent (arctangent) and obeys the subtraction identity:

$$\text{atan}(A) - \text{atan}(B) = \text{atan} \frac{A - B}{1 + AB}. \quad (\text{S4})$$

One of the results (I_1) was previously obtained by Pan[26] and is closely related to Eq.(3.26) in the work by Smith[3]; we have not found any evaluation of I_2 in the literature.

A. Preliminary Integrals

Before proceeding to the derivations, we list several preliminary definite integrals used throughout the evaluations, valid for $x, t, \tau > 0$:

$$\int_0^x \frac{du \tau}{u^2 + \tau^2} = \text{atan}(x/\tau), \quad (\text{S5})$$

$$\int_0^x \frac{du (u^2 + t^2)^{-1}}{\sqrt{u^2 + t^2 + \tau^2}} = \frac{1}{t\tau} \text{atan} \frac{\tau x}{t\sqrt{x^2 + t^2 + \tau^2}}, \quad (\text{S6})$$

$$\int_0^x \frac{du}{(u^2 + \tau^2)^{3/2}} = \frac{x}{\tau^2 \sqrt{\tau^2 + x^2}}, \quad (\text{S7})$$

$$\int_0^x \frac{du}{(u^2 + \tau^2)^{5/2}} = \frac{3\tau^2 x + 2x^3}{3\tau^4(\tau^2 + x^2)^{3/2}}, \quad (\text{S8})$$

$$\int_0^x \frac{du}{(u^2 + \tau^2)^{7/2}} = \frac{15\tau^4 x + 20\tau^2 x^3 + 8x^5}{15\tau^6(\tau^2 + x^2)^{5/2}}, \quad (\text{S9})$$

$$\int_0^x \frac{du u^2}{(u^2 + \tau^2)^{7/2}} = \frac{5\tau^2 x^3 + 2x^5}{15\tau^4(\tau^2 + x^2)^{5/2}}, \quad (\text{S10})$$

$$\int_0^x \frac{du (11 + 7u^2)}{(1 + u^2)^3(2 + u^2)^{5/2}} = \\ \frac{x(2x^6 + 10x^4 + 17x^2 + 11)}{2(x^2 + 1)^2(x^2 + 2)^{3/2}}. \quad (\text{S11})$$

Eq. (S6) can be derived via the Euler substitution $w = u + \sqrt{u^2 + t^2 + \tau^2}$ which rationalizes the square root and reduces the integral to a standard arctangent form. Eqs. (S7) to (S11) were obtained via an ansatz method: assuming an antiderivative of the form $P(u)/Q(u)$, where $Q(u)$ matches the

expected denominator structure, then determining the coefficients of the polynomial $P(u)$ by differentiation and matching. We also list a number of definite integrals involving the error function defined as

$$\operatorname{erf}(\tau) = \frac{2}{\sqrt{\pi}} \int_0^\tau du e^{-u^2}. \quad (\text{S12})$$

$$\int_{-\infty}^{\infty} du e^{-tu^2} \frac{\sin(u\tau)}{u} = \pi \operatorname{erf}\left(\frac{\tau}{2\sqrt{t}}\right), \quad (\text{S13})$$

$$\int_0^{\infty} du \frac{\operatorname{erf}(u\tau)u}{e^{u^2}} = \frac{1}{2} \frac{\tau}{\sqrt{1+\tau^2}}, \quad (\text{S14})$$

$$\int_0^{\infty} du \frac{\operatorname{erf}(ut)\operatorname{erf}(u\tau)}{e^{u^2}} = \frac{1}{\sqrt{\pi}} \operatorname{atan} \frac{t\tau}{\sqrt{1+\tau^2+t^2}}, \quad (\text{S15})$$

$$\int_{-\infty}^{\infty} du e^{-tu^2} \sin(u\tau)u = \frac{\sqrt{\pi}\tau}{2\sqrt{t^3}} e^{-\tau^2/(4t)}. \quad (\text{S16})$$

Eqs. (S13) to (S15) can be derived by parametric differentiation: differentiating with respect to τ yields simpler expressions, which are integrated and then antidifferentiated back to recover the full result. Eq. (S16) follows from differentiating Eq. (S13) with respect to t .

B. Derivation of I_1 via the divergence theorem

To evaluate the volume integral in Eq. (S1), we apply the divergence theorem (also known as Gauss's theorem). First, observe the identity

$$\begin{aligned} (\mathbf{r} \cdot \nabla_{\mathbf{x}})^2 |\mathbf{x}|^{-1} &= \nabla_{\mathbf{x}} \cdot \left[\mathbf{r} \left(\mathbf{r} \cdot \nabla_{\mathbf{x}} |\mathbf{x}|^{-1} \right) \right] \\ &= -\nabla_{\mathbf{x}} \cdot \left[\mathbf{r} (\mathbf{r} \cdot \mathbf{x}) |\mathbf{x}|^{-3} \right], \end{aligned} \quad (\text{S17})$$

since $\nabla_{\mathbf{x}} |\mathbf{x}|^{-1} = -\mathbf{x}/|\mathbf{x}|^3$. Using this identity, the volume integral can be transformed into a surface integral over the boundary $\partial\Omega(a, b, c)$ of the cuboid:

$$I_1 = -\frac{1}{2} \oint_{\partial\Omega(a,b,c)} \mathbf{r} \cdot d\mathbf{S} \frac{\mathbf{r} \cdot \mathbf{x}}{|\mathbf{x}|^3}, \quad (\text{S18})$$

where $d\mathbf{S}$ denotes an infinitesimal vector element of surface area, directed outward from the enclosed volume.

The cuboid has six faces—three pairs of opposite rectangles lying in planes parallel to the xy , yz , and zx coordinate planes, respectively. Considering the face at $x_3 = +c/2$ whose outward normal is $+\mathbf{e}_3$. On this face, $d\mathbf{S} = dx_1 dx_2 \mathbf{e}_3$ and $\mathbf{x} = (x_1, x_2, c/2)$, so

$$\mathbf{r} \cdot d\mathbf{S} (\mathbf{r} \cdot \mathbf{x}) = dx_1 dx_2 (xz x_1 + yz x_2 + z^2 c/2). \quad (\text{S19})$$

Due to the even symmetry of the integration domain $[-a/2, a/2] \times [-b/2, b/2]$ in both x_1 and x_2 , the terms

linear in x_1 or x_2 integrate to zero. Only the term proportional to z^2 survives. On the opposite face at $x_3 = -c/2$, the outward normal is $-\mathbf{e}_3$, giving $\mathbf{r} \cdot d\mathbf{S} (\mathbf{r} \cdot \mathbf{x}) = dx_1 dx_2 (-xzx_1 - yzx_2 + z^2 c/2)$ and again yielding a non-zero contribution only from the z^2 term upon integration. Thus, the total contribution from the pair of faces ($x_3 = \pm c/2$) doubles the surviving quadratic term. Analogous reasoning applies to the other two pairs of faces. Hence, the full integral becomes

$$I_1 = z^2 S_{xy} + x^2 S_{yz} + y^2 S_{zx}, \quad (\text{S20})$$

where S_{xy} , S_{yz} , and S_{zx} denote the coefficients of the quadratic terms contributed by the pair of faces parallel to the xy -, yz -, and zx -planes, respectively. Explicitly,

$$S_{xy} = \int_{-a/2}^{a/2} dx_1 \int_{-b/2}^{b/2} dx_2 \frac{-c/2}{(x_1^2 + x_2^2 + c^2/4)^{3/2}}. \quad (\text{S21})$$

Exploiting evenness in x_1 and x_2 and using the substitutions $u = 2x_1$ and $v = 2x_2$, we obtain

$$\begin{aligned} S_{xy} &= -4c \int_0^a du \int_0^b dv \frac{1}{(u^2 + v^2 + c^2)^{3/2}} \\ &= -4bc \int_0^a du \frac{1}{u^2 + c^2} \frac{1}{\sqrt{u^2 + b^2 + c^2}}, \end{aligned} \quad (\text{S22})$$

where the integration over dv is of the form in Eq. (S7). Applying Eq. (S6) to the remaining integral yields

$$\begin{aligned} S_{xy} &= -4 \operatorname{atan} \frac{ab}{c\sqrt{a^2 + b^2 + c^2}} \\ &= -4 \operatorname{atan} \frac{1}{\xi_3 \sqrt{\xi_1^2 + \xi_2^2 + \xi_3^2}}. \end{aligned} \quad (\text{S23})$$

By symmetry, the other two pairs of faces contribute

$$S_{yz} = -4 \operatorname{atan} \frac{1}{\xi_1^2 \sqrt{\xi_1^2 + \xi_2^2 + \xi_3^2}}, \quad (\text{S24})$$

and

$$S_{zx} = -4 \operatorname{atan} \frac{1}{\xi_2^2 \sqrt{\xi_1^2 + \xi_2^2 + \xi_3^2}}, \quad (\text{S25})$$

respectively. Summing all contributions yields the desired result in Eq. (S1). Using the subtraction identity in Eq. (S4) and noting that $\xi_1 \xi_2 \xi_3 = 1$, one finds,

$$S_{xy} + S_{yz} + S_{zx} = -2\pi. \quad (\text{S26})$$

C. Derivation of I_1 via the Fourier transform

Instead of employing the divergence theorem, the integral

$$I_1(\mathbf{r}, 2a, 2b, 2c) = \frac{1}{2} \int_{\Omega(2a, 2b, 2c)} d\mathbf{x} (\mathbf{r} \cdot \nabla_{\mathbf{x}})^2 \frac{1}{|\mathbf{x}|} \quad (\text{S27})$$

can be evaluated using Fourier transform techniques. Here, $\Omega(2a, 2b, 2c) = [-a, a] \times [-b, b] \times [-c, c]$ denotes a cuboid of side lengths $2a$, $2b$, and $2c$, which shares the same aspect ratio (i.e., shape) as $\Omega(a, b, c)$. As shown below, the integration yields the same result as in Eq. (S1). We begin with the inverse Fourier transform:

$$\frac{1}{|\mathbf{x}|} = \frac{1}{8\pi^3} \int_{\mathbb{R}^3} d\mathbf{k} e^{i\mathbf{k}\cdot\mathbf{x}} \frac{4\pi}{k^2}, \quad (\text{S28})$$

where $\mathbf{k} = (k_1, k_2, k_3)$ and $k^2 = |\mathbf{k}|^2 = k_1^2 + k_2^2 + k_3^2$. Taking two derivatives gives

$$(\mathbf{r} \cdot \nabla_{\mathbf{x}})^2 \frac{1}{|\mathbf{x}|} = -\frac{1}{2\pi^2} \int_{\mathbb{R}^3} d\mathbf{k} e^{i\mathbf{k}\cdot\mathbf{x}} \frac{(\mathbf{r} \cdot \mathbf{k})^2}{k^2}, \quad (\text{S29})$$

and then interchanging the order of integrations yields

$$I_1 = -\frac{1}{4\pi^2} \int_{\mathbb{R}^3} d\mathbf{k} \frac{(\mathbf{r} \cdot \mathbf{k})^2}{k^2} \left[\int_{\Omega(2a, 2b, 2c)} d\mathbf{x} e^{i\mathbf{k}\cdot\mathbf{x}} \right]. \quad (\text{S30})$$

The inner integral factorizes:

$$\int_{\Omega(2a, 2b, 2c)} d\mathbf{x} e^{i\mathbf{k}\cdot\mathbf{x}} = \frac{\sin(k_1 a)}{k_1/2} \frac{\sin(k_2 b)}{k_2/2} \frac{\sin(k_3 c)}{k_3/2}, \quad (\text{S31})$$

which is even in k_1 , k_2 and k_3 . To handle the $1/k^2$ term, we use the identity from a Gaussian integral:

$$\frac{1}{k^2} = \int_0^\infty dw e^{-k^2 w} = \int_0^\infty dw e^{-k_1^2 w} e^{-k_2^2 w} e^{-k_3^2 w}. \quad (\text{S32})$$

Substituting Eqs. (S31) and (S32) into Eq. (S30) allows us to write I_1 as a four-dimensional integral, three over $d\mathbf{k} = dk_1 dk_2 dk_3$ and one over dw . Expanding $(\mathbf{r} \cdot \mathbf{k})^2 = x^2 k_1^2 + y^2 k_2^2 + z^2 k_3^2 + \text{cross terms}$, we observe that all cross terms (e.g. $k_1 k_2$) integrate to zero due to odd symmetry under $k_1 \rightarrow -k_1$ etc. Thus,

$$I_1 = x^2 C_x + y^2 C_y + z^2 C_z, \quad (\text{S33})$$

where each coefficient arises from integrating one quadratic component. The integrals over $d\mathbf{k}$ factorize and can be evaluated using Eqs (S13) and (S16). For example, for the x^2 -term:

$$C_x = \int_0^\infty \frac{dw}{\sqrt{w^3}} \frac{a}{e^{a^2/(4w)}} \text{erf}\left(\frac{b/2}{\sqrt{w}}\right) \text{erf}\left(\frac{c/2}{\sqrt{w}}\right). \quad (\text{S34})$$

Now applying the substitution $2\sqrt{w} = a/u$, so that

$$\frac{dw}{\sqrt{w^3}} = 4 \frac{du}{a}; \quad \frac{a^2}{4w} = u^2; \quad \frac{b}{2\sqrt{w}} = \frac{b}{a}u; \quad \text{etc.} \quad (\text{S35})$$

and

$$C_x = -4\sqrt{\pi} \int_0^\infty du e^{-u^2} \text{erf}\left(u \frac{b}{a}\right) \text{erf}\left(u \frac{c}{a}\right). \quad (\text{S36})$$

Under this change of variables, the integral in C_x now matches the form of Eq. (S15) with $t = b/a$ and $\tau = c/a$, yielding $C_x = S_{yz}$ (see Eq. (S24)). By symmetry, C_y and C_z are

obtained analogously (e.g., exchanging $a \leftrightarrow b$ in C_x gives $C_y = S_{zx}$, and $a \leftrightarrow c$ gives $C_z = S_{xy}$). Thus, Eq. (S33) recovers the result in Eq. (S20) or (S1).

This alternative derivation has certain advantages. For example, from Eqs. (S30), (S31) and the Dirichlet integral

$$\int_{-\infty}^\infty du \frac{\sin(u\tau)}{u} = \pi; \quad \text{for } \tau > 0, \quad (\text{S37})$$

it follows that the sum of the coefficients is shape-independent:

$$C_x + C_y + C_z = -2\pi. \quad (\text{S38})$$

This property is not immediately apparent in the previous derivation via the divergence theorem.

For the purpose of deriving the shape-dependent term for a macroscopic rectangular prism, Smith arrived at his Eq.(3.26) in Ref.[3], which equals the negative of Eq. (S36). He wrote, “in spite of some diligent work, no analytic progress has been made with (3.26).” The closed-form expressions for the integrals (Eqs. (S14) and (S15) obtained by parametric differentiation) thus resolve this analytic challenge. The connection between the shape-dependent term and $I_1(\mathbf{r})$ is also transparent. The usual shape-dependent terms are always non-negative[2, 3]. The one obtained by Smith is written in terms of the total dipole moment[3]:

$$J(\mathbf{M}) = -\frac{1}{V} (C_x M_x^2 + C_y M_y^2 + C_z M_z^2), \quad (\text{S39})$$

where $V = l_x l_y l_z$ is the volume of the unit cell, and the total dipole moment for a unit cell containing N charges is defined as

$$\mathbf{M} = (M_x, M_y, M_z) = \sum_{j=1}^N q_j \mathbf{r}_j. \quad (\text{S40})$$

The infinite boundary term $\nu_{\text{ib}}(\mathbf{r}) = I_1(\mathbf{r})/V$ is directly related to $J(\mathbf{M})$ via the following pairwise sum[18, 19]

$$\sum_{i < j}^N q_i q_j \nu_{\text{ib}}(\mathbf{r}_i - \mathbf{r}_j) = J(\mathbf{M}) - \frac{q_{\text{tot}}}{V} \sum_{j=1}^N q_j |\mathbf{r}_j|^2, \quad (\text{S41})$$

where $q_{\text{tot}} = \sum_{j=1}^N q_j$ is the total charge. For a neutral system ($q_{\text{tot}} = 0$), the second term vanishes, and the pairwise sum reduces exactly to $J(\mathbf{M})$.

D. Derivation of I_2 via the divergence theorem

To derive the integral

$$I_2(\mathbf{r}, a) = \frac{1}{24} \int_{\Omega(a, a, a)} d\mathbf{x} (\mathbf{r} \cdot \nabla_{\mathbf{x}})^4 \frac{1}{|\mathbf{x}|}, \quad (\text{S42})$$

we first rescale the coordinates via $\mathbf{x} \rightarrow \mathbf{x}a/2$, mapping the original cube onto the centro-symmetric domain $\Omega(2, 2, 2) =$

$[-1, 1]^3$ of side length 2. After scaling, the integral simplifies to

$$I_2(\mathbf{r}, a) = \frac{4}{a^2} I_2(\mathbf{r}, 2) = \frac{1}{a^2} I_0(\mathbf{r}), \quad (\text{S43})$$

where

$$I_0(\mathbf{r}) = \frac{1}{6} \int_{\Omega(2,2,2)} d\mathbf{x} (\mathbf{r} \cdot \nabla_{\mathbf{x}})^4 \frac{1}{|\mathbf{x}|}. \quad (\text{S44})$$

This a^{-2} scaling implies $I_2(\mathbf{r}, a) \rightarrow 0$ as $a \rightarrow \infty$, confirming that I_2 constitutes a finite-size correction to the bulk (infinite-domain) limit. Below we derive the explicit form

$$I_0(\mathbf{r}) = \frac{24r^4 - 40(x^4 + y^4 + z^4)}{9\sqrt{3}}, \quad (\text{S45})$$

in analogy with the derivation of I_1 , using the divergence theorem.

We employ the identity

$$(\mathbf{r} \cdot \nabla_{\mathbf{x}})^4 \frac{1}{|\mathbf{x}|} = 3\nabla_{\mathbf{x}} \cdot \left[\frac{3r^2(\mathbf{r} \cdot \mathbf{x})}{|\mathbf{x}|^5} \mathbf{r} - \frac{5(\mathbf{r} \cdot \mathbf{x})^3}{|\mathbf{x}|^7} \mathbf{r} \right], \quad (\text{S46})$$

and apply the theorem to obtain

$$I_0 = \frac{1}{2} \oint_{\partial\Omega(2,2,2)} \mathbf{r} \cdot d\mathbf{S} \left[\frac{3r^2(\mathbf{r} \cdot \mathbf{x})}{|\mathbf{x}|^5} - \frac{5(\mathbf{r} \cdot \mathbf{x})^3}{|\mathbf{x}|^7} \right]. \quad (\text{S47})$$

Consider the face at $x_3 = +1$ (normal $+\mathbf{e}_3$). On this face:

$$\mathbf{r} \cdot d\mathbf{S} = dx_1 dx_2 z; \quad \mathbf{x} = (x_1, x_2, +1), \quad (\text{S48})$$

and the integration domain for $dx_1 dx_2$ is the square $[-1, 1]^2$, symmetric under $x_1 \rightarrow -x_1$ and $x_2 \rightarrow -x_2$. In the expansion of $\mathbf{r} \cdot \mathbf{x} = x_1 x_2 + z$, terms odd in x_1 or x_2 vanish upon integration. Thus only the constant term z survives in $\mathbf{r} \cdot \mathbf{x}$. For $(\mathbf{r} \cdot \mathbf{x})^3$, we have

$$(\mathbf{r} \cdot \mathbf{x})^3 = z^3 + 3z(x^2 x_1^2 + y^2 x_2^2) + \text{odd terms}. \quad (\text{S49})$$

Furthermore, the square domain possesses exchange symmetry between x_1 and x_2 . Using this symmetry and $x^2 + y^2 = r^2 - z^2$, the combination $x^2 x_1^2 + y^2 x_2^2$ may be replaced—upon integration—by $(r^2 - z^2)x_2^2$ (or equivalently by $(r^2 - z^2)x_1^2$). Thus, up to terms that integrate to zero,

$$(\mathbf{r} \cdot \mathbf{x})^3 \rightarrow z^3 + 3z(r^2 - z^2)x_2^2. \quad (\text{S50})$$

By symmetry, the contributions from opposite faces are equal. Summing the contributions from all six faces, we write

$$I_0 = D_{xy} + D_{yz} + D_{zx}, \quad (\text{S51})$$

where, for instance, D_{xy} denotes the combined contribution of the two faces parallel to the xy -plane ($x_3 = \pm 1$). Explicitly,

$$D_{xy} = 4r^2 z^2 (J_5 - K_2) - 4z^4 (J_7 - K_2), \quad (\text{S52})$$

with the auxiliary integrals

$$J_5 = \int_0^1 dx_1 \int_0^1 dx_2 \frac{3}{(x_1^2 + x_2^2 + 1)^{5/2}}, \quad (\text{S53})$$

$$J_7 = \int_0^1 dx_1 \int_0^1 dx_2 \frac{5}{(x_1^2 + x_2^2 + 1)^{7/2}}, \quad (\text{S54})$$

and

$$K_2 = \int_0^1 dx_1 \int_0^1 dx_2 \frac{15x_2^2}{(x_1^2 + x_2^2 + 1)^{7/2}}. \quad (\text{S55})$$

The factor of 4 in Eq. (S52) arises from exploiting evenness in x_1 and x_2 to restrict the double integral to the quadrant $[0, 1]^2$.

Carrying out the integrations over dx_2 (using Eqs. (S8) to (S10)) yields

$$J_5 - K_2 = \int_0^1 dx_1 \frac{3}{(2 + x_1^2)^{5/2}} = \frac{2}{3\sqrt{3}}, \quad (\text{S56})$$

and

$$J_7 - K_2 = \int_0^1 dx_1 \frac{22 + 14x_1^2}{3(1 + x_1^2)^3 (2 + x_1^2)^{5/2}} = \frac{10}{9\sqrt{3}}, \quad (\text{S57})$$

where the remaining integrals are evaluated analytically using Eqs. (S8) and (S11). Substituting Eqs. (S56) and (S57) into Eq. (S52) gives

$$D_{xy} = \frac{24r^2 z^2 - 40z^4}{9\sqrt{3}}, \quad (\text{S58})$$

and cyclic permutation yields

$$D_{yz} = \frac{24r^2 x^2 - 40x^4}{9\sqrt{3}}; \quad D_{zx} = \frac{24r^2 y^2 - 40y^4}{9\sqrt{3}}. \quad (\text{S59})$$

Substituting these results into Eq. (S51) yields the expression stated in Eq. (S45), completing the derivation. Finally, using $r^4 = x^4 + y^4 + z^4 + 2(x^2 y^2 + y^2 z^2 + z^2 x^2)$, the result may be recast as an alternative linear combination of quadrupolar invariants:

$$I_0 = \frac{80(x^2 y^2 + y^2 z^2 + z^2 x^2) - 16r^4}{9\sqrt{3}}. \quad (\text{S60})$$

We have explicitly evaluated the integral over the cubic domain and expressed the result as linear combinations of quadrupolar terms. For a general cuboid domain, the same structural form holds, with coefficients given by analogous double integrals; however, their explicit evaluation is more involved and lies beyond the scope of this work.